STATE FEEDBACK CONTROLLER DESIGN APPLIED TO QUADRATIC BOOST CONVERTER USED IN PHOTOVOLTAIC ARRAY MPPT

Gabriel Morais, Ernane A. A. Coelho
NUPEP
UFU
Uberlândia, Brazil
gabrielmorais_12@hotmail.com, ernane@ufu.br

Ernane A. A. Coelho
NUPEP
UFU
Uberlândia, Brazil
gabrielmorais_12@hotmail.com, ernane@ufu.br

Eric Nery Chaves
NuPSE
IFG
Itumbiara, Brazil
eric.neryx@gmail.com, ghunterp@gmail.com

Ghunter Paulo Viajante
NuPSE
IFG
Itumbiara, Brazil
eric.neryx@gmail.com, ghunterp@gmail.com

Rafael Nielson
Enel Goiás
Goiânia, Brazil

***Abstract* — This paper presents the controller design that will be used in the internal loop of the maximum power point tracking (MPPT) algorithm to control the output voltage of a PV (photovoltaic) array. The PV system is intended to be connected to the single-phase power grid through the DC-DC Quadratic Boost converter at the interface between the PV panels and the DC bus. The proposed controller uses the state feedback technique and, in its design, it will be demonstrated the mathematical modeling of the DC-DC Quadratic Boost converter, the step-by-step determination of the discrete gains that feed the plant, and computational simulation results that show the viability of the control technique in question and corroborate its use.**

Keywords—Maximum Power Point Tracking, Photovoltaic Generation, Quadratic Boost Converter, State Feedback Control.

I. INTRODUCTION

The efficiency in the conversion of electrical energy in distributed generation systems composed by photovoltaic panels is limited to approximately 14 to 16% in the best conditions of irradiance and temperature [1]. This efficiency depends on the point of the IxV curve, characteristic of PV (photovoltaic) panels, in which the system is operating. This point of operation depends on the voltage and current at the output terminals of the PV array, and since the load fed by the photo-generated energy has an eminently changeable profile, it is necessary to interface this load with the PV array through a DC-DC converter.

A DC-DC converter typically used in this application is the Boost converter in which the static gain is defined by:

$$\frac{V_{OUT}}{V_{IN}} = \frac{1}{1-D} \tag{1}$$

D is the duty cycle of the converter switch, 0 < D < 1. However, the Boost converter has performance limitations when scanned in regions close to D = 1 [2]. In this context, the Quadratic Boost converter becomes an option to be able to raise voltages at higher values without considerable loss of efficiency, since the conversion factor of the input voltage, V_{IN}, to the output voltage, V_{OUT}, is greater than that of the Boost converter [3]. The static gain of the DC-DC Boost Quadratic converter is shown in (2).

$$\frac{V_{OUT}}{V_{IN}} = \frac{1}{(1-D)^2} \tag{2}$$

Typically, this converter is used to obtain a stabilized output voltage, even with variations of the input voltage or load [4]. However, for maximum power extraction applications in photovoltaic arrays, the input voltage is the variable to be controlled, and the output voltage is considered a constant value, since the output of the converter will be connected in parallel to a fixed DC bus. Thus, the circuit is analyzed as shown in Figure 1.

It can be noted that the input of the converter is a resistor of variable resistance, R_{PV}, that models the variations of voltage and current provided by the photovoltaic array, depending on the local irradiance and temperature. The mathematical modeling of this converter is necessary so that controllers can be designed for

the variables of the internal loop (voltage Vc_1 or current i_{PV}) of the algorithms that aim to extract the maximum power of the PV array.

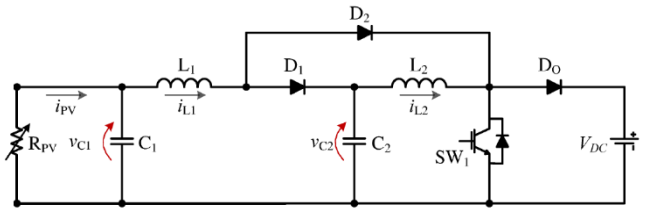

Fig. 1. Modified Structure of the Quadratic Boost Converter for application in photovoltaic systems.

In general terms, the P&O-MPPT (perturb and observe maximum power point tracking) algorithm used in this work determines, dynamically, the voltage of the photovoltaic array that would provide the maximum power available from the environmental conditions at that time. From this value, a controller seeks to change the duty cycle of the SW_1 switch, so that the input voltage Vc_1 of the converter is maintained at the reference voltage, given by the MPPT logic, at the same time that is boosted to the stabilized output voltage value V_{DC}.

Therefore, the objective of this paper is to present the controller design that will be used in the internal loop of the P&O-MPPT algorithm to control the output voltage of a photovoltaic array. The PV system is intended to be connected to the single-phase power grid and has the DC-DC Quadratic Boost converter at the interface between the PV panels and the DC bus.

For this same DC-DC Quadratic Boost converter in this type of application (MPPT), in [5] a PID compensator was used, added to the action of a Notch filter, and in [6] a controller based on the internal model with a degree of freedom (IMC-1DOF), both designed to control the input voltage of said DC-DC converter.

In this paper, the proposed controller uses the state feedback technique and, in its design, will be demonstrated the mathematical modeling of the DC-DC Quadratic Boost converter, the step-by-step determination of discrete gains that feed the plant and results of computational simulation that show the viability of the control technique in question and corroborate its use.

II. Mathematical Modeling of Quadratic Boost Converter

Since Quadratic Boost converter, in continuous conduction mode (CCM) has two distinct operating stages - I, for switch SW_1 conducting and II for switch SW_1 blocked – it is needed to find the state space mathematical model of each stage and average them, considering the period in which each step is active. The mathematical model by state space consists of representing linear systems by two temporal equations, the system and the output, namely:

$$\dot{x}(t) = Ax(t) + Bu(t) \tag{3}$$

$$y(t) = Cx(t) + Eu(t) \tag{4}$$

The chosen states are the currents in each inductor and the voltages in each capacitor. Thus,

$$x = \begin{bmatrix} i_{L_1} & i_{L_2} & v_{C_1} & v_{C_2} \end{bmatrix}^T \tag{5}$$

The system input vector u(t) is the V_{DC} voltage at the output of the DC-DC Quadratic Boost converter.

A. *Analysis of voltages and currents in the first stage of operation*

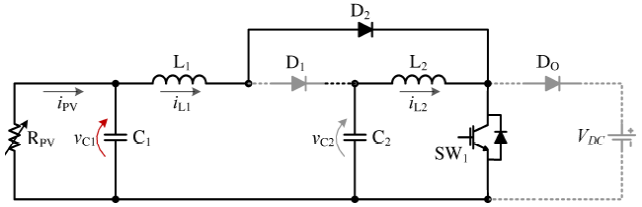

Fig. 2. Quadratic Boost Converter operation step 1.

In Step 1, shown in Figure 2, the switch SW_1 and the diode D_2 conduct, and the diodes D_1 and D_0 are reverse polarized. The linear equations that describe this step are:

$$\dot{x} = A_1 x + B_1 u \tag{6}$$

$$y = C_1 x + E_1 u \tag{7}$$

From the analysis of circuits via Kirchhoff's Laws:

$$A_1 = \begin{bmatrix} 0 & 0 & \frac{1}{L_1} & 0 \\ 0 & 0 & 0 & \frac{1}{L_2} \\ -\frac{1}{C_1} & 0 & -\frac{1}{C_1 R_{PV}} & 0 \\ 0 & -\frac{1}{C_2} & 0 & 0 \end{bmatrix} \tag{8}$$

$$B_1 = \begin{bmatrix} 0 & 0 & 0 & 0 \end{bmatrix}^T \tag{9}$$

$$C_1 = \begin{bmatrix} 0 & 0 & 1 & 0 \end{bmatrix} \tag{10}$$

$$E_1 = 0 \tag{11}$$

B. *Analysis of voltages and currents in the second stage of operation*

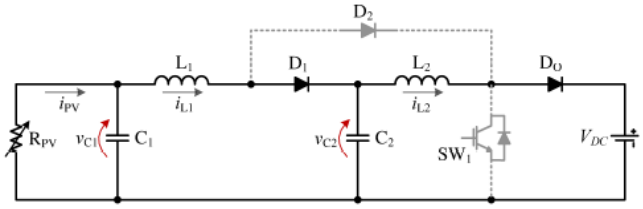

Fig. 3. Quadratic Boost Converter operation step 2

In Step 2, shown in Figure 3, the switch SW_1 and the diode D_2 are blocked, and the diodes D_1 and D_0 conduct. The linear equations that describe this step are:

$$\dot{x} = A_2 x + B_2 u \tag{12}$$

$$y = C_2 x + E_2 u \tag{13}$$

From the analysis of circuits via Kirchhoff's Laws:

$$A_2 = \begin{bmatrix} 0 & 0 & \frac{1}{L_1} & -\frac{1}{L_1} \\ 0 & 0 & 0 & \frac{1}{L_2} \\ -\frac{1}{C_1} & 0 & -\frac{1}{C_1 R_{PV}} & 0 \\ \frac{1}{C_2} & -\frac{1}{C_2} & 0 & 0 \end{bmatrix} \tag{14}$$

$$B_2 = \begin{bmatrix} 0 & -\frac{1}{L_2} & 0 & 0 \end{bmatrix}^T \tag{15}$$

$$C_2 = \begin{bmatrix} 0 & 0 & 1 & 0 \end{bmatrix} \tag{16}$$

$$E_2 = 0 \tag{17}$$

The converter can be represented by matrices obtained through the average between the matrices of each step, considering the time within the conducting period in which each one is valid. So,

$$A_{med} = A_1 D + A_2 (1 - D) \tag{18}$$

$$B_{med} = B_1 D + B_2 (1 - D) \tag{19}$$

$$C_{med} = C_1 D + C_2 (1 - D) \tag{20}$$

$$E_{med} = E_1 D + E_2 (1 - D) \tag{21}$$

Since this system is nonlinear, it is necessary to perform its linearization by choosing a point of operation in a steady state in which the derivatives of the state equations are zero. Hence, the system represented in the form of equation (3) can be represented by equation (22).

$$\dot{X}_{med} = A_{med} X_{med} + B_{med} U_{med} \tag{22}$$

After some algebra in (22), considering $\dot{X}_{med} = 0$ in steady state, it is obtained (23):

$$X_{med} = -A_{med}^{-1} B_{med} U_{med} \tag{23}$$

Thus, the average state vector becomes (24):

$$X_{med} = \begin{bmatrix} x_1 & x_2 & x_3 & x_4 \end{bmatrix}^T \tag{24}$$

Where

$$x_1 = -\frac{V_{DC}(1-D)^2}{R_{PV}} \tag{25}$$

$$x_2 = -\frac{V_{DC}(1-D)^3}{R_{PV}} \tag{26}$$

$$x_3 = V_{DC}(1-D)^2 \tag{27}$$

$$x_4 = V_{DC}(1-D) \tag{28}$$

Considering that the system will operate around the point of equilibrium, it is necessary to model the small variation dynamics of the system around this point, those variations in the duty cycle and their effects on the input voltage. In this way, the states, the input vector and the duty cycle are analyzed as containing their average value, plus a small signal of time-varying perturbation. The model of small signals is applied to the state and output equations, simplifications are made and the Laplace transform is applied to obtain (29).

$$\tilde{X}(s) = (sI - A_{med})^{-1} \left[B_{med} \tilde{U}(s) + B_d \tilde{D}(s) \right] \tag{29}$$

Where

$$B_d = [A_1 - A_2] X_{med} + [B_1 - B_2] V_{DC} \tag{30}$$

Considering that there is no variation of the input U(s) of the system, $\tilde{U}(s) = 0$. Writing the transfer function of the variations of the states in relation to the variation of duty cycle, it is obtained (32):

$$\frac{\tilde{X}(s)}{\tilde{D}(s)} = (sI - A_{med})^{-1} \left\{ A_{sub} X_{med} + B_{sub} V_{DC} \right\} \tag{31}$$

Where

$$A_{sub} = A_1 - A_2 \tag{32}$$

$$B_{sub} = B_1 - B_2 \tag{33}$$

Being this system of fourth-order and one input, the expression (31) is a 4x1 column matrix. Desiring to control the disturbance of the input voltage of the converter, here represented by $\tilde{v}_{C_1}$, in relation to the disturbance in the duty cycle $\tilde{d}$, the desired transfer function is

$$G_{\tilde{v}_{C_1} / \tilde{d}}(s) = \frac{a_2 s^2 + a_1 s + a_0}{b_4 s^4 + b_3 s^3 + b_2 s^2 + b_1 s + b_0} \tag{34}$$

Where

$$a_2 = -V_{DC}(1-D)(R_{PV}C_2L_2) \quad (35)$$

$$a_1 = V_{DC}(1-D)^3 L_2 \quad (36)$$

$$a_0 = -2V_{DC}(1-D)R_{PV} \quad (37)$$

$$b_4 = R_{PV}C_1L_1C_2L_2 \quad (38)$$

$$b_3 = L_1L_2C_2 \quad (39)$$

$$b_2 = R_{PV}[C_1L_1 + C_2L_2 + C_1L_2(1-D)^3] \quad (40)$$

$$b_1 = L_1 + L_2(1-D)^2 \quad (41)$$

$$b_0 = R_{PV} \quad (42)$$

C. *Presentation of the electrical parameters*

The inductance and capacitance values available for carrying out the work are such that L_1 = 982 mH, L_2 = 1986 mH, $C_1 = C_2$ = 4.77 µF. The DC bus at the output of the converter is such that V_{DC} = 100 V. The average duty cycle that raises the maximum power voltage from 61.2 V to 100 V, through (2), is D = 0.212. The value of R_{PV}, being a model for the photovoltaic arrangement, is given by (43).

$$R_{PV} = \frac{V_{MPP}^{\ 2}}{P_{MPP}} \quad (43)$$

The photovoltaic array used provides a voltage of 62.10 V for a 540 W maximum power. Table 1 shows the specifications of each of the two panels that were connected in series, valid values for 1000 W/m² irradiance and 25 ° C.

TABLE I. ELECTRICAL PARAMETERS OF EACH PHOTOVOLTAIC PANELL

Model	Risen RSM60-6-270P
Maximum Power	270 W
Open-circuit voltage	37.90 V
Open-circuit current	9.20 A
Voltage at maximum power	31.05 V
Current at maximum power	8.70 A
Efficiency	16 %

Thus, at the point of operation adopted, R_{PV} = 7.14 Ω. The parameters of the voltage perturbation transfer function in the input capacitor of the converter relative to the disturbance in the switch duty cycle for the given electrical parameters are shown in Table II.

TABLE II. PARAMETERS OF THE TRANSFER FUNCTION GIVEN IN (36)

a_2	-6.498×10^{-6}
a_1	0.09719
a_0	-1370
b_4	3.863×10^{-16}
b_3	9.312×10^{-12}
b_2	1.744×10^{-7}
b_1	0.00215
b_0	8.696

III. OPEN-LOOP SYSTEM ANALYSIS

A mathematical software allows to obtain the system response to the unitary step, shown in Figure 4, where one can se a certain oscillation in high frequency, caused by two open-loop complex conjugated poles that have a high imaginary part, in addition to the inversion of the temporal response, caused by two zeros in the right half-plane. In addition, the settling time (time required for the signal to enter the ± 2% of steady state value for the last time) is around 1ms.

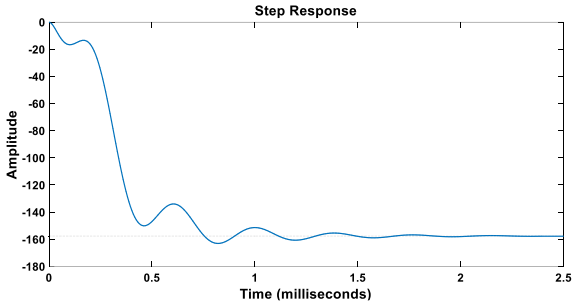

Fig. 4. Open-loop system response to unitary step.

IV. DISCRETE INTEGRAL CONTROL WITH STATE FEEDBACK

Figure 5 shows the discrete block diagram of the system consisting of integral controller + plant + state feedback.

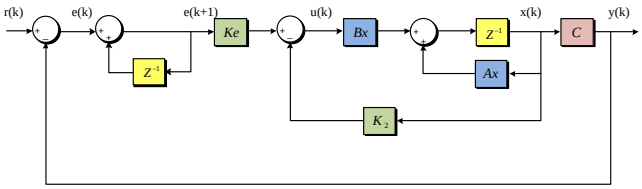

Fig. 5. Block diagram of system (integral controller, state feedback and plant).

Discrete Integral Control consists in determining the values of the row-matrix K and the constant Ke such that the closed-loop poles of the system are the ones that provide the desired dynamics for the output. Integral control is necessary because it raises the system type, zeroing the steady-state error for step inputs of plants that do not contain any integrators in the path of forward action, as it is in this case, evidenced by (36). As a consequence of this control, there is the increase of the order of the system by 1. One way to determine the K and Ke gains is by using the Ackermann Formula with some modifications for discrete systems. The step-by-step of the determination of (44) is shown in [7]. Equations (44) to (49) are made considering that the systems are represented in the controller canonical form and that they are of 4th order.

$$[K_{1,4} \quad K_e] = [\hat{K} + [\vec{0}_{1,4} \quad 1]] \begin{bmatrix} G - I_4 & H \\ CG & CH \end{bmatrix}^{-1} \quad (44)$$

Where

$$\hat{K} = [\vec{0}_{1,4} \quad 1] W_c^{-1} \phi(\hat{A}) \quad (45)$$

$$W_c = [\hat{B} \quad \hat{A}\hat{B} \quad \hat{A}^2\hat{B} \quad \hat{A}^3\hat{B} \quad \hat{A}^4\hat{B}] \tag{46}$$

$$\hat{A} = \begin{bmatrix} G & H \\ \vec{0}_{1,4} & 0 \end{bmatrix} \tag{47}$$

$$\hat{B} = \begin{bmatrix} \vec{0}_{4,1} \\ 1 \end{bmatrix} \tag{48}$$

$\phi(\hat{A})$ is the closed-loop discrete characteristic equation for z = Â. G and H are the discrete system and input matrices, respectively, represented in the controller canonical form.

$$\phi(\hat{A}) = \hat{A}^5 + \alpha_1 \hat{A}^4 + \alpha_2 \hat{A}^3 + \alpha_3 \hat{A}^2 + \alpha_4 \hat{A} + \alpha_5 I_5 \tag{49}$$

The coefficients α are given after determination of the closed-loop poles. The discrete representation of the closed-loop system is given by (50).

$$\begin{bmatrix} x(k+1) \\ e(k+1) \end{bmatrix} = t \begin{bmatrix} x \\ e \end{bmatrix} \tag{50}$$

Where

$$t = \begin{bmatrix} G & H \\ K_{1,4} - K_{1,4}G - K_e CG & 1 - K_{1,4}H - K_e CH \end{bmatrix} \tag{51}$$

The eigenvalues of the matrix t shown in (51) are the poles of the closed-loop system (CL). Knowing that K_{1x4} gains are found for systems represented in the controller canonical form, a similarity transformation is needed to find K_2, which are the corresponding K_{1x4} values that bring the current system represented in any other form to have the CL poles given by the eigenvalues of t. This is done through (52).

$$K_2 = K_{1,4}\left[tW_c^{-1}\right]^{-1} \tag{52}$$

Where t is the controllability matrix of the open-loop plant represented in its original form and W_C is the controllability matrix of the open-loop plant represented in the controller canonical form.

The great advantage of this controller is to allow the closed-loop poles, as long as they lead to a stable system, to be allocated arbitrarily. However, one does not have control over the saturation of the control effort. Empirically, it is known that when designing a control that requires controlled response with dynamics not much faster than the open loop one, the control action will not saturate. Computational simulations are necessary at the designing stage of performance criteria to ensure that the control effort is within acceptable limits.

V. Definition of the Desired Performance of the Response and Determination of Feedback Gains

The controller of this plant must be capable of stabilizing the input voltage of the Quadratic Boost DC-DC converter at an inferior time than the reference change given by the MPPT algorithm operating at 50 Hz, i.e., less than 20 ms. The closed-loop settling time of 1 ms was adopted. The response adopted for the output had the Bessel Type dynamics, which presents little overshoot and adjustable settling time. Figure 6 shows the Bessel response for systems of order 1 to 5 with settling time of 1 second.

The continuous poles providing the 5th order dynamics shown in Figure 6 are -6.4480; -4.1104 ± j6.3142; -5.9268 ± j3.0813 rad/s. They should be divided by 1 ms so that the response will have a settling time of 1 ms. In addition, one must have to map them to z-plane by applying (53) to find the discrete characteristic closed-loop equation given by (49). The choice of the sampling period T must be made in accordance with the Nyquist's Theorem, in other words, T ⩽ 2Ta, where Ta is the smaller period of the signal. An empirical way of choosing T is so that it is 6 to 10 times smaller than the settling time of the signal. Thus, T should be between 0.1 ms and 0.16 ms. However, being more conservative, a T of 0.0025 ms was chosen.

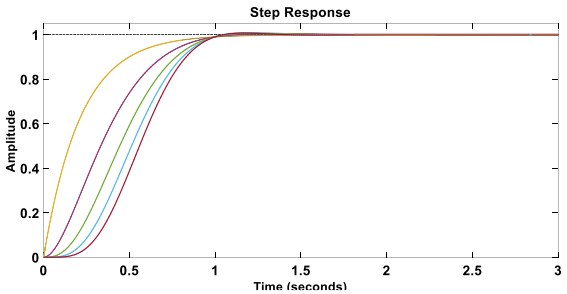

Fig. 6. Bessel Type Response for 1st to 5th order systems.

$$z = e^{sT} \tag{53}$$

In this way, after the due calculations, the values of the array-line K_2 and the constant Ke are obtained: K_2 = [0.06777; -0.07129; 0.002312; -0.001159] and Ke = -0.0001127.

VI. Computational Simulation Results

The MPPT algorithm used was the Perturb and Observe (P&O) algorithm. To validate the operation of the control, a time-varying irradiance profile was created in the range of 200 W/m² to 1000 W/m², with a temperature of 25 °C, to be implemented in PV panels. Figure 7 shows the output dynamics compared to the reference voltage, given by the MPPT algorithm.

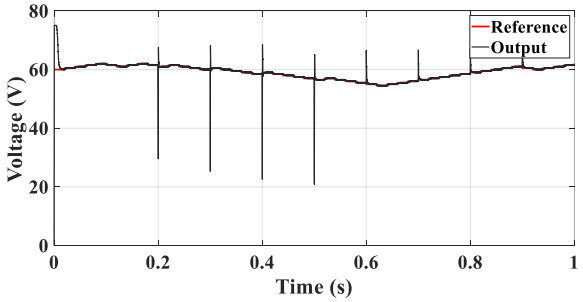

Fig. 7. Comparison of the output signal with the reference.

It is possible to note certain voltage variations at times multiple of 0.1 seconds, which is when steps of 200 W/m² in the irradiance were chosen to be made in simulation. It is worth mentioning that these abrupt variations of climatic conditions were simulated only to ascertain the effectiveness of the control and they are hardly repeated in practice.

Figure 8 shows an enlargement of Figure 7 in the range of 0.06 seconds to 0.14 seconds. In it, it can be seen that the input voltage dynamics meets the design criteria determined in section V.

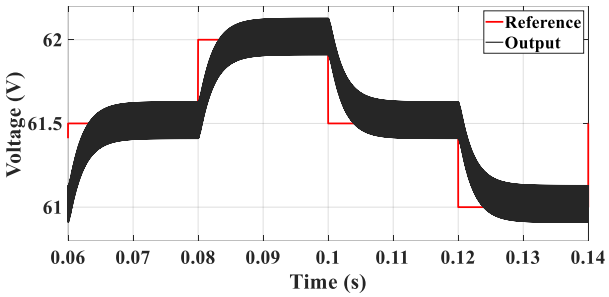

Fig. 8. Amplification of Figure 7 in the time range from 0.06 seconds to 0.14 seconds.

Figure 9 shows the comparison of the maximum power that could be delivered by the photovoltaic arrangement to that extracted by the DC-DC converter. From it, one can see the efficiency of the control in extracting the maximum power available by the array.

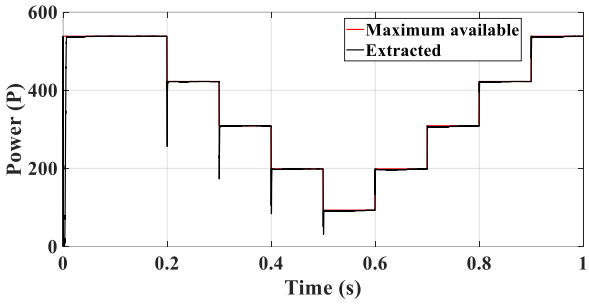

Fig. 9. Comparison of the maximum power available by the photovoltaic array to the extracted power.

Figure 10 shows an enlargement of Figure 9 in the period of 0.2 seconds to 0.3 seconds. The voltage reference step used in the MPPT algorithm in simulation was 0.5 V. Representing a small percentage - 0.8% - of the maximum power voltage V_{MPP} - 61.2 V - it is noticed that, in steady state, there is little oscillation around the maximum available power at the moment. However, for abrupt variations of irradiance, MPP tracking is slower.

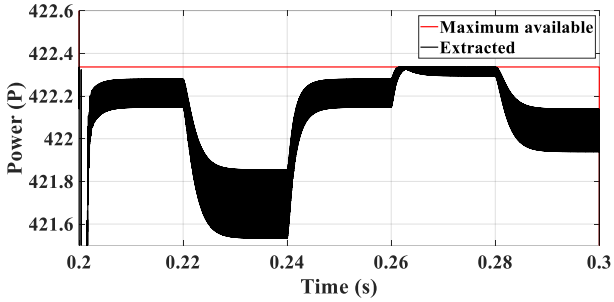

Fig. 10. Amplification of Figure 9 in the time range of 0.2 to 0.3 seconds.

VII. Conclusion

Mathematical modeling using an average state space, followed by linearization around an operating point, allowed one to analyze the behavior of the system when subjected to disturbances in the switch duty cycle. This model allowed to identify the location of the poles and zeros in the open-loop of the plant, evidencing that it has its own dynamics that cannot be easily controlled by traditional techniques. From the mathematical model, a discrete integral controller was designed by state feedback, which allowed to allocate the closed-loop poles where they guarantee a desired transient response and which made it possible to bring to zero the steady-state error between the given reference voltage by the MPPT algorithm and the input voltage of the Quadratic Boost converter. The desired closed-loop poles were chosen from the standard Bessel Type response, which presents little overshoot and adjustable settling time, and the responses obtained in a computational simulation attest the location of these poles, thus validating the suggested technique of control.

References

[1] SNYMAN, D. B., ENSLIN, J. H. R., “An experimental evaluation of MPPT converter topologies for PV installations”. Renewably Energy, vol. 3, issue 8, pp. 841-848, 1993.

[2] D. Maksimovic, S. Cuk, *“Switching converters with wide DC conversion range”*, IEEE Transactions on Power Electronics, vol. 6, no.1, pp. 151–157, janeiro 1991.

[3] L. H. S. C. Barreto, *Análise, projeto e desenvolvimento de conversores para a concepção de uma UPS online não isolada*, Tese de Doutorado, Universidade Federal de Uberlândia - UFU, Uberlândia-MG, Brasil, 2003.

[4] M. L. Kumari, S. Bhattacharya and U. S. Triar, "*Stabilization of boost converter with output filter using LQR based state-feedback controller*," 2016 10th International Conference on Intelligent Systems and Control (ISCO), Coimbatore, 2016, pp. 1-6.

[5] R. A. S. Carvalho, L. S. Vilefort, F. V. R. Silva, L. C. G. Freitas, E. A. A. Coelho, L. C. FREITAS, J. B. VIEIRA JR., *“Estudo do Conversor Boost Quadrático para Rastreamento de Máxima Potência em Sistemas Fotovoltaicos Utilizando o Método Perturba & Observa”*, Conferência de Estudos em Engenharia Elétrica, UFU, 2014.

[6] R. A. S. Carvalho, L. S. Vilefort, F. V. R. Silva, L. C. G. Freitas, E. A. A. Coelho, L. C. FREITAS, J. B. VIEIRA JR., *“Estudo do Conversor Boost Quadrático para Rastreamento de Máxima Potência em Sistemas Fotovoltaicos Utilizando o Método Perturba & Observa”*, Conferência de Estudos em Engenharia Elétrica, UFU, 2014.

[7] K. Ogata, *Discrete-time Control Systems*, Prentice-Hall International, 2nd edition, New Jersey, 1995.